Proc. Indian Acad. Sci. (*Chem. Sci.*), Vol. 115, Nos 5 & 6, October–December 2003, pp 321–332

Rigid rod spaced fullerene as building block for nanoclusters[¶]

PALLIKARA K SUDEEP[1], JAMES P VARKEY[1], K GEORGE THOMAS*[1], MANAPPURATHU V GEORGE*[,1] and PRASHANT V KAMAT*[2]
[1]Photosciences and Photonics Division, Regional Research Laboratory, Thiruvananthapuram 695 019, India
[2]Radiation Laboratory, University of Notre Dame, IN 46556, USA
e-mail: kgt@vsnl.com; mvgeorge@rediffmail.com; pkamat@nd.edu

Abstract. By using phenylacetylene based rigid-rod linkers (PhA), we have successfully synthesized two fullerene derivatives, C_{60}–PhA and C_{60}–PhA–C_{60}. The absorption spectral features of C_{60}, as well as that of the phenylacetylene moiety are retained in the monomeric forms of these fullerene derivatives, ruling out the possibility of any strong interaction between the two chromophores in the ground state. Both the fullerene derivatives form optically transparent clusters, absorbing in the UV-Vis region; this clustering leads to a significant increase in their molar extinction coefficients. TEM characterization of the C_{60}–PhA showed large spherical clusters, with sizes ranging from 150–350 nm, while an elongated wire-type structure was observed for the *bis*fullerene derivative (C_{60}–PhA–C_{60}). AFM section analysis studies of isolated nanoclusters of C_{60}–PhA–C_{60}, deposited on mica, indicate that smaller clusters associate to form larger nanostructures.

Keywords. Fullerenes; nanoclusters; AFM and TEM studies.

1. Introduction

Nature has crafted biological designs having unquestionable superiority in architecture and chemists have been exploring the basic principles behind such self-assembly and also the possibilities of crafting similar systems.[1–4] The key to such design strategy is our ability to organise simple molecular building blocks to nanostructured systems, adopting the principle of inter- as well as intramolecular interactions (for e.g. hydrogen bonding, van der Waal/electrostatic forces, hydrophobic/hydrophilic interactions).[4] Supramolecular chemistry offers numerous possibilities for such designs. Recently, the design of highly symmetric cages of nanometre dimensions through coordination driven self-assembly has been reported.[4] Interestingly, the dimensions of these nanoscopic complexes can even extend into the range of proteins, having large internal cavities. These aspects were reviewed recently by Seideland and Stang.[4]

The nanoclusters derived from inorganic materials such as transition metals,[5–7] semiconductors,[5,8,9] and silica[10–13] have been used for designing organized nanostructured assemblies. In contrast, very little is known about the mechanism of the formation of nanoparticles of organic molecules and their properties, although diversity allows greater possibilities. Fullerenes form optically transparent and thermodynamically stable clusters.[14–20] Recent investigations from our group have revealed that C_{60}-based systems,

[¶]Dedicated to Professor C N R Rao on his 70th birthday
*For correspondence

for example, monofunctionalized as well as *bis*- and *tris*-fullerenes form optically transparent clusters of different nanostructural arrangements in mixed solvents (acetonitrile/toluene), depending on the number of the fullerene molecules present.[21] For example, monofunctionalized fullerene derivatives form spherical clusters (~ 170 nm), whereas the *bis*- and *tris*-fullerene derivatives form nanostructures, with sizes ranging from 100 nm to 1 *m*m and shapes varying from elongated wires to entangled spheres. The C_{60} units, in both the *bis*- as well as *tris*-fullerene derivatives, are linked together by flexible alkyl groups and hence several modes of interactions are possible for these systems due to the existence of a wide range of conformations, leading to different shapes. By taking advantage of the clustering behaviour of C_{60}, we have demonstrated a novel approach for charge stabilization.[19–21] Compared to the monomeric form of fullerene-aniline dyads, the laser excitation of the clustered dyads yield remarkably stable charge transfer products, with lifetimes of several hundred microseconds. The close network of fullerene moieties in the cluster facilitates the hopping of electron from the parent fullerene to the adjacent molecule, thus increasing the spatial distance between the charge-separated pairs. It may be interesting to note that both *bis*- and *tris*-fullerene clusters possess a better charge stabilizing ability, compared to the clusters of monofunctionalized systems. With a view to achieving well-defined and organized nanostructures from fullerene-based systems, we have examined a mono (C_{60}–PhA) and a *bis*-fullerene derivative (C_{60}–PhA–C_{60}), connected to rigid rod linkers, involving phenylacetylene units.

2. Experimental section

2.1 *Methods*

All melting points are uncorrected and were determined on an Aldrich melting point apparatus. ^{1}H NMR and ^{13}C NMR spectra were recorded on a Bruker DPX-300 MHz spectrometer. Mass spectra were recorded on a JOEL JM AX 5505 HA mass spectrometer. The UV-Vis spectra were recorded on a Shimadzu 2401 or 3101PC spectrophotometer. The emission spectra were recorded on a Spex-Fluorolog, F112-X equipped with a 450 W Xe lamp and a Hamamatsu R928 photomultiplier tube. A 570 nm long pass filter was placed before the emission monochromator in order to eliminate the interference from the solvent. The spectra were corrected in each case by subtracting the solvent spectra. Dynamic light scattering studies were carried using a Coulter model N4 plus particle analyser. Transmission electron micrographs were recorded using a Hitachi H600 transmission electron microscope by applying a drop of the colloid sample on carbon coated copper grid. AFM images were recorded using a Digital Nanoscope IIIa in tapping mode. An etched silicon tip was used as an AFM probe for imaging the samples.

2.2 *General method of synthesis*

The general method adopted for the synthesis of the monofullerene (C_{60}–PhA) and the *bis*fullerene (C_{60}–PhA–C_{60}) derivatives, with rigid-rod linkers is shown in scheme 1. Compounds **2–5** were prepared by adopting methods similar to the reported procedures.[22,23] We have adopted a different procedure for the preparation of the dialdehyde (**6**), by treating the corresponding phenylacetylene derivative, **5** with 4-bromobenzaldehyde.

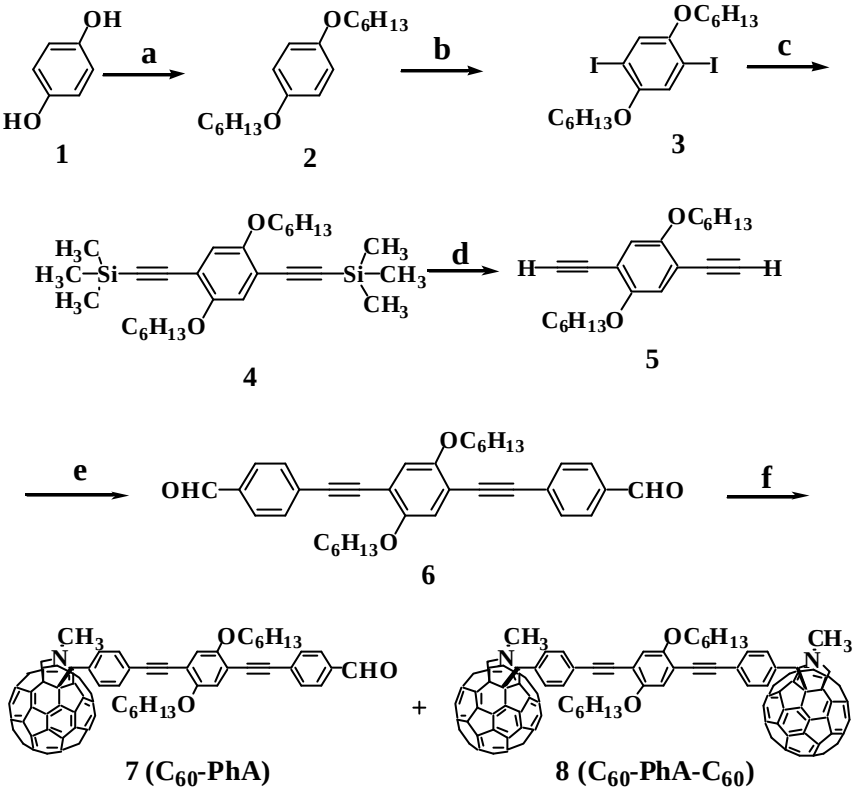

Scheme 1. (a) $C_6H_{13}Br$, KOH, ethanol, reflux; (b) KIO_3, I_2, AcOH, H_2SO_4; (c) trimethyl-silylacetylene, $Pd(PPh_3)_2Cl_2$, CuI, diisopropylamine, reflux; (d) NaOH, methanol, THF; (e) BrC_6H_4CHO, $Pd(PPh_3)_4$, diisopropylamine, toluene; (f) C_{60}, sarcosine, toluene, reflux.

The syntheses of both C_{60}–PhA (**7**) and C_{60}–PhA–C_{60} (**8**) were achieved through a 1,3-dipolar cycloaddition reaction of the azomethine ylide, generated through the reaction of the aldehyde **6** and N-methylglycine, with C_{60} (scheme 1), following a general procedure adopted by Prato *et al* for the synthesis of functionalised fullerenes.[24,25] All new compounds were fully characterised on the basis of analytical results and spectral data.

2.2a *Synthesis of* **6***:* A mixture of **5** (100 mg, 0·310 mM), 4-bromobenzaldehyde (125 mg, 0·678 mM), $Pd(PPh_3)_4$ (14·2 mg, 0·012 mM) and CuI (2·35 mg, 0·012 mM) was added to a degassed solution of diisopropylamine (4 ml) in toluene (9 ml). The mixture was heated to 80°C for 24 h. After cooling to room temperature, it was added dropwise into a vigorously stirred solution of methanol. The precipitate was collected and chromatographed over silica gel, using toluene as eluent to give **6** (73 mg, 45%) as a yellow solid. ^{1}H NMR ($CDCl_3$, 300 MHz) δ 10·24 (*s*, 2H, CHO), 7·78–7·81 (*d*, 2H, aromatic), 7·59–7·61 (*d*, 2H, aromatic), 6·96 (*s*, 2H, aromatic), 3·96 (*t*, 4H, OCH_2), 1·24–1·8 (*m*, 22H, alkyl protons); ^{13}C NMR ($CDCl_3$, 75 MHz) δ 191·38, 153·85, 135·42, 132·02, 129·66, 129·57, 116·83, 113·90, 94·24, 94·00, 69·60, 31·557, 29·25, 25·73, 22·62, 14·01; exact mass calculated for $C_{36}H_{38}O_4$ ($M^{\cdot+}$) 534·2270, found 534·2758 (FAB high resolution mass spectrometry).

2.2b *Synthesis of the fullerene derivatives: C_{60}–PhA (**7**) and C_{60}–PhA–C_{60} (**8**)* – A mixture of C_{60} (270 mg, 0·374 mM), sarcosine (33·7 mg, 0·374 mM) and **6** (100 mg, 0·187 mM) was heated under argon in toluene (270 ml) for 30 h. The solvent was removed under reduced pressure and the crude product was chromatographed over silica gel (100–200 mesh). Elution with a mixture of (1 : 1) of hexane and toluene gave 120 mg (42%) of unchanged C_{60} followed by 15 mg of the bisadduct **8** (C_{60}–PhA–C_{60}), and 15 mg of the monoadduct **7** (C_{60}–PhA).

Monofunctionalised fullerene C_{60}–PhA (**7**) – m.p. > 400°C; ^{1}H NMR ($CDCl_3 + CS_2$) δ 9·95 (*s*, 1H, CHO), 7·79–7·73 (*m*, 4H, aromatic), 7·57–7·48 (*m*, 4H, aromatic), 6·89–6·88 (*d*, 2H, aromatic), 4·90–4·95 (*m*, 2H, pyrrolidine ring CH_2), 4·23 (*d*, 1H, pyrrolidine ring CH), 3·91 (*t*, 4H, OCH_2), 2·78 (*s*, 3H, NCH_3), 0·88–1·77 (*m*, 22H, alkyl protons); ^{13}C NMR ($CS_2 + CDCl_3$) δ 190·45, 153·44, 153·00, 146·07, 145·25, 142·11, 142·04, 141·91, 131·86, 131·79, 129·34, 129·15, 125·75, 116·77, 115·13, 114·82, 114·47, 113·06, 112·41, 111·95, 111·25, 110·93, 110·11, 108·86, 107·968, 107·63, 107·19, 106·82, 106·44, 101·57, 99·42, 83·22, 69·46, 69·328, 39·86, 31·64, 29·35, 25·81, 23·57, 22·78, 14·12; The mass spectrum of C_{60}–PhA (**7**) showed an [$M^{\cdot+}$] peak at 1281 (FAB mass spectrometry).

Bisfullerene C_{60}–PhA–C_{60} (**8**) – m.p. > 400°C; ^{1}H NMR ($CDCl_3 + CS_2$) δ 7·73 (*s*, 4H, aromatic), 7·47 (*d*, 4H, aromatic), 6·8 (*s*, 2H, aromatic), 4·90–4·95 (*m*, 4H, pyrrolidine ring CH_2), 4·23 (*d*, 2H, pyrrolidine ring CH), 3·91 (*t*, 4H, OCH_2), 2·78 (*s*, 6H, NCH_3), 0·88–1·77 (*m*, 22H, alkyl protons); ^{13}C NMR ($CS_2 + CDCl_3$) δ 155·70, 153·24, 152·545, 146·98, 146·02, 145·95, 145·91, 145·88, 145·83, 145·79, 145·69, 145·63, 145·42, 145·29, 145·08, 145·05, 144·98, 144·93, 144·87, 144·39, 144·35, 144·07, 142·85, 142·80, 142·32, 142·29, 141·97, 141·93, 141·84, 141·79, 141·73, 141·59, 141·38, 141·27, 139·90, 139·69, 139·34, 136·78, 136·59, 136·24, 135·60, 135·42, 131·62, 131·47, 128·92, 123·69, 117·09, 116·46, 114·72, 113·79, 112·50, 95·28, 94·72, 87·26, 83·02, 69·78, 69·24, 69·07, 68·65, 39·72, 31·65, 29·81, 29·38, 29·21, 25·81, 25·75, 22·86, 14·18.

3. Results and discussion

The general methods adopted for the syntheses of the mono and the *bis*fullerene derivatives have been discussed in §2. Dipolar cycloaddition reaction of azomethine ylides, generated through the reaction of the *bis*aldehyde (**6**) and N-methylglycine, with C_{60} (scheme 1) yielded two products, namely, the monofunctionalized fullerene derivative (C_{60}–PhA) and the *bis*fullerene derivative, (C_{60}–PhA–C_{60}). Photophysical characterization of the monomeric forms of the fullerene derivatives (C_{60}–PhA and C_{60}–PhA–C_{60}) and their clustering properties are presented here. Morphology, as well as the size of the clustered forms of the fullerene derivatives were carried out using transmission electron microscopy (TEM) and tapping mode atomic force microscopy (TM-AFM).

3.1 *Monomers of fullerene derivatives*

Photophysical as well as clustering behavior of both fullerene derivatives were compared with (**6**), containing the phenylacetylene based linker group. Normalized absorption spectra of C_{60}, the dialdehyde (**6**) and the fullerene derivatives (C_{60}–PhA and C_{60}–PhA–C_{60}) are presented in figure 1. In toluene, compound **6** possess two well-separated bands,

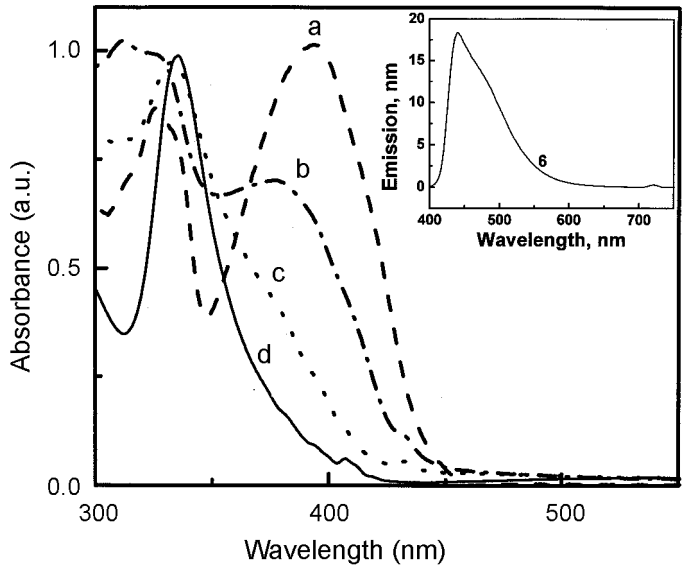

Figure 1. Normalised absorption spectra of (a) the *bis*aldehyde (**6**); (b) the monofullerene derivative (C_{60}–PhA); (c) the *bis*fullerene derivative (C_{60}–PhA–C_{60}) and (d) C_{60}. Inset shows the emission spectrum of the *bis*aldehyde in toluene (excitation wavelength: 360 nm).

with absorption maxima at 327 and 393 nm respectively. The latter band can be clearly seen as a shoulder in both the fullerene derivatives, though it is less dominant for the *bis*fullerene (C_{60}–PhA–C_{60}), when compared to the monofunctionalized derivative, C_{60}–PhA. The spectral features of isolated chromophores are more or less retained in the case of the monofullerene derivative, ruling out the possibility of any strong interaction between the two chromophores in the ground state. In the case of the bisfullerene (C_{60}–PhA–C_{60}), the absorption band corresponding to phenylacetylene based linker may be buried in the broad absorption of fullerene units. The emission spectra of the fullerene derivatives (C_{60}–PhA and C_{60}–PhA–C_{60}) exhibit two well-separated bands (excitation wavelength 300 nm) with maxima around 455 and 710 nm respectively. It may be noted that fullerene derivatives emit around 710 nm and the short wavelength band arises from the phenylacetylene-based linker group (inset of figure 1). Currently, we are involved in the synthesis of *bis*fullerene derivatives, possessing phenylacetylenes of varying length, in order to investigate the possibility of photoinduced energy as well as electron transfer processes. These aspects will be discussed in a later paper.

3.2 *Computational studies*

With a view to examining the conformational features of the fullerene adducts, we have carried out the molecular modelling calculation of a representative example, such as the *bis*fullerene (C_{60}–PhA–C_{60}), using Titan software. The equilibrium geometry was estimated using AM1 calculation. The energy-minimized conformation obtained through molecular modelling calculation is shown in figure 2. In the case of C_{60}–PhA–C_{60}, the

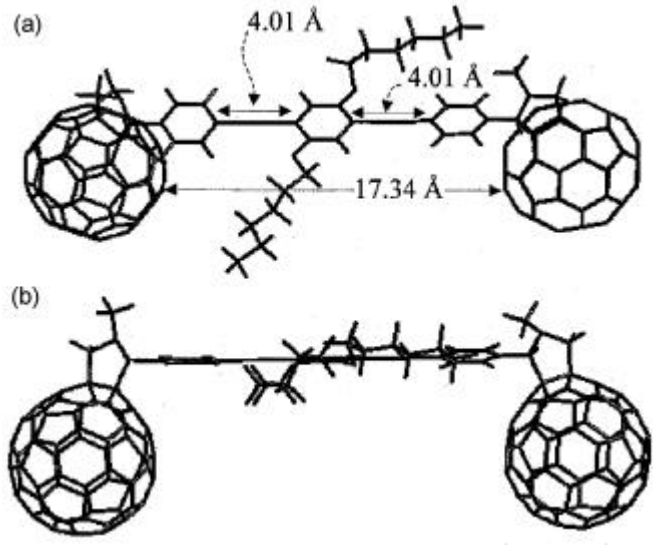

Figure 2. Energy-minimised conformation of *bis*fullerene derivative, C_{60}–PhA–C_{60}; (**a**) All the phenyl groups lie in the same plane and (**b**) the fullerene units lie in a plane orthogonal to the plane of the phenyl groups.

distance of separation between the two C_{60} units is found to be 17·39 Å. It is interesting to note that all the three phenyl groups lie in a plane, which is orthogonal to the plane containing the fullerene units. Such a linear structure of the *bis*fullerene, may favour a linear stacking, leading to wire type clusters, on aggregation.

3.3 *Characterisation of clusters of fullerene derivatives*

Fullerene derivatives are highly soluble in nonpolar solvents such as toluene. In polar solvents, clustering minimises the nonpolar surface of C_{60} exposing to a polar environment. As demonstrated earlier, such a configuration is achieved through three-dimensional hydrophobic interactions between molecules.[18–21,26] In the present case, both the fullerene derivatives possess strong absorption in the UV region with extended tail absorption ranging to the visible region. We have investigated the clustering behaviour of the fullerene derivatives (C_{60}–PhA and C_{60}–PhA–C_{60}) in a mixture (1 : 19) of toluene/acetonitrile (figures 3 and 4), by injecting the toluene solution of the fullerene derivative into acetonitrile, by adopting a 'fast addition method'. In a nonpolar solvent such as toluene, both the compounds obey Beer–Lambert law, up to a concentration range of 0·1 mM (inset of figure 4), ruling out the possibility of cluster formation. Absorption spectra of the fullerene derivatives (C_{60}–PhA and C_{60}–PhA–C_{60}), in toluene and toluene/acetonitrile were compared at a constant substrate concentration, in each case. The absorption spectra of the clusters turned featureless with a significant increase in molar extinction coefficient, in each case. These clusters were quite stable at room temperature and could be reverted to the corresponding monomer forms by increasing the fraction of the nonpolar solvent. The effect of clustering on the emission spectra of fullerene derivatives was investigated and the spectral properties of the monomer as well

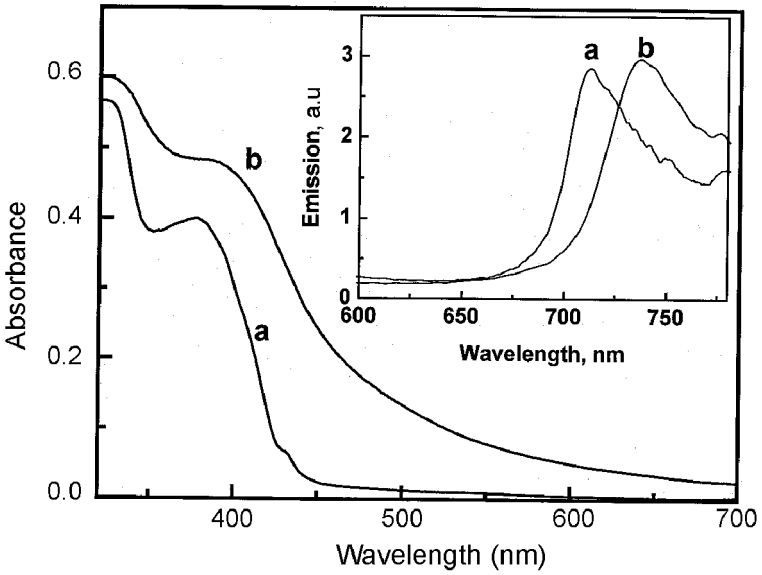

Figure 3. Absorption spectra of fullerene derivative, C_{60}–PhA (31·5 *m*M) in (a) toluene and (b) toluene/acetonitrile. Inset shows the normalised emission spectra of the fullerene derivative, C_{60}–PhA in (a) toluene and (b) toluene/acetonitrile (1 : 19).

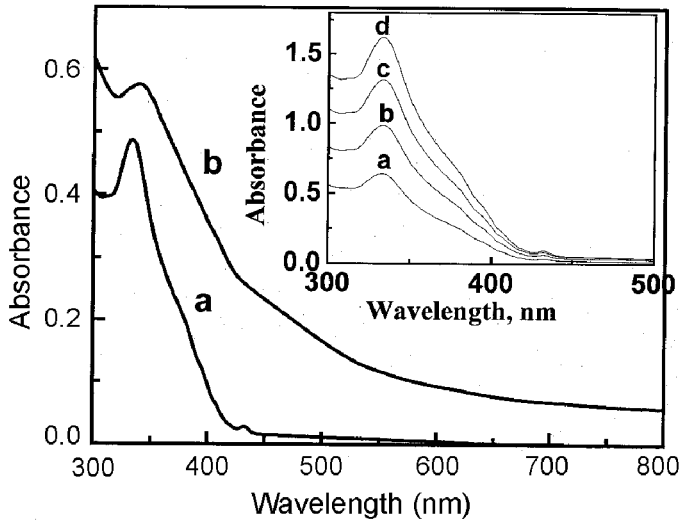

Figure 4. Absorption spectra of the *bis*fullerene, C_{60}–PhA–C_{60} (31·5 *m*M) in (a) toluene and (b) toluene/acetonitrile (1 : 19). Inset shows the absorption spectra of C_{60}–PhA–C_{60} at different concentrations in toluene.

as of the cluster are presented in table 1. For both the fullerene derivatives, it was observed that clustering leads to a bathochromic shift and a representative example (C_{60}–PhA) is shown in the inset of figure 3. The clusters of fullerene derivatives were further

characterized using dynamic light scattering measurements. The average cluster diameter for C_{60}–PhA and C_{60}–PhA–C_{60} were 220 and 260 nm respectively and both these clusters showed a large cluster size distribution. In order to understand the shape of the clusters of fullerene derivatives, TEM studies were further carried out.

TEM images of the clusters of C_{60}–PhA and C_{60}–PhA–C_{60}, deposited on carbon grid are shown in figure 5. Clusters of C_{60}–PhA and C_{60}–PhA–C_{60} exhibited two different types of clustering behaviour (Note that the clusters were prepared from the mixture of (1 : 49) toluene/acetonitrile). The monofunctionalized fullerene derivative (C_{60}–PhA) forms large spherical clusters with size ranging from 150–350 nm. Interestingly, a different type of structural feature was observed for *bis*fullerene clusters. The *bis*fullerene clusters (C_{60}–PhA–C_{60}) deposited on the carbon grid showed an elongated wire type structure with closely linked spherical fullerene clusters, having a smaller size distribution compared to C_{60}–PhA. In our earlier studies, the formation of spherical clusters was observed in the case of monofunctionalized fullerene derivatives, whereas elongated wire type nanostructures were seen for the *bis*fullerene clusters.[21] Based on these observations, it can be concluded that the way with which the mono as well as the *bis*fullerenes stack themselves to form clusters is different. The energy-minimized

Table 1. Absorption and emission properties of monomers and clusters.

Compound	Solvent	Extinction coefficient (470 nm)	l_{max}, nm (em)
7	Toluene	430	713
7	Toluene/acetonitrile	5800	737
8	Toluene	460	714
8	Toluene/acetonitrile	6520	737

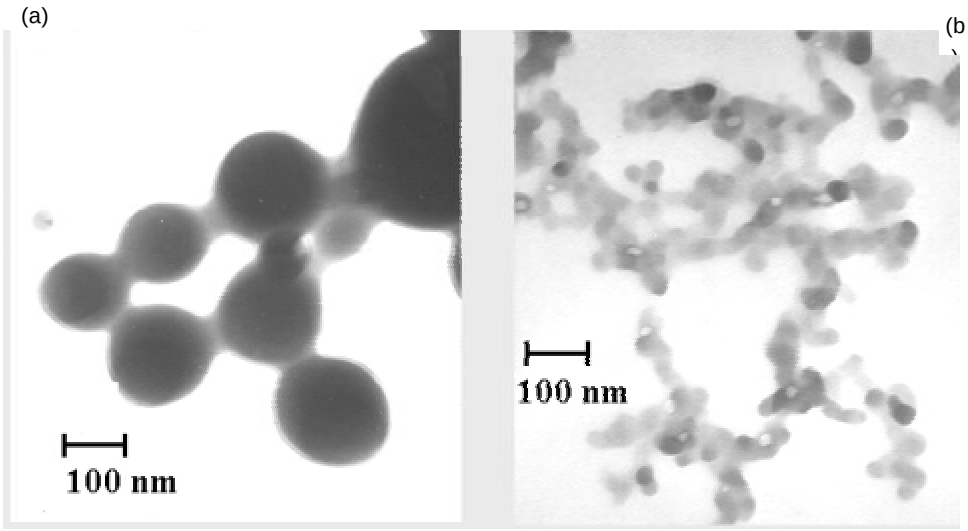

Figure 5. Transmission electron micrographs of the clusters of (**a**) the mono-fullerene derivative (C_{60}–PhA) and (**b**) the *bis*fullerene derivative (C_{60}–PhA–C_{60}).

conformation for the *bis*fullerene (C_{60}–PhA–C_{60}), obtained through molecular model calculation indicates that both the fullerene units lie in the same plane and are held together by the rigid rod linker group. Such a dumbbell-shaped molecular structure can favour linear stacking, through the interaction with C_{60} units of another molecule, as evidenced from TEM studies.

For obtaining further insight on the morphology of the nanoclusters, detailed AFM studies were carried out. Recent AFM studies have shown that the morphology of nanoparticles can be tuned by varying the environment (solvents, additives that can act as templates such as polymers, micellar systems etc.).[27–29] More recently, independent work from two different groups has shown that in the absence of additives, porphyrin derivatives form small nanoparticles with narrow size distribution,[30] whereas template-directed self-assembly of a structurally similar porphyrin derivative, using poly-L-lysine, yields large rodlike structures.[29] Various methods of AFM sample preparation were reported recently for environmentally important biopolymers such as humic acid, polysaccharides etc. and it may be noted that the sample preparation also plays a major role in the morphology of clusters.[30,31] In the present study, images were collected using a

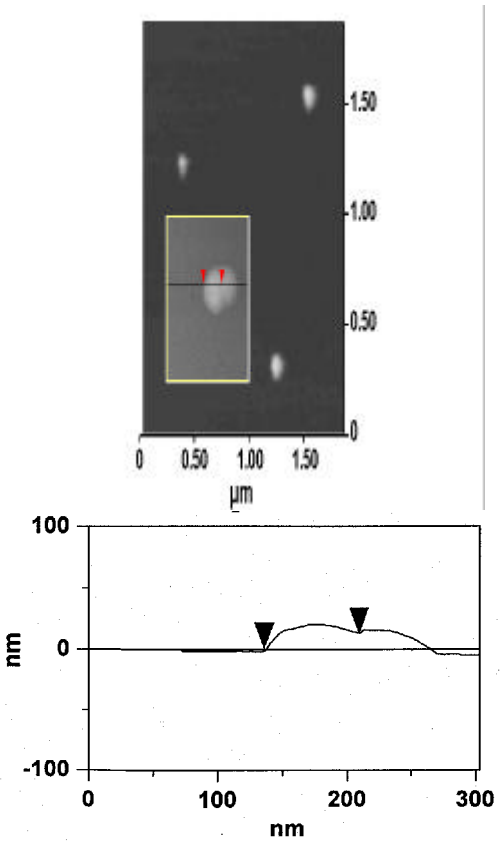

Figure 6. AFM image (*z* range: 200 nm) and sectional analysis of the mono-functionalized fullerene derivative (C_{60}–PhA) assembled on a mica sheet (5 *m*l of 17 *m*M cluster solution was transferred to a mica sheet of 1 × 1 cm).

tapping mode AFM (TM-AFM), since this method is more suited for studying soft organic samples. Silicon tips with a resonance frequency of approximately 350 kHz were used in tapping mode. Specimens were prepared by adding 10–40 μl of cluster suspension (concentration of fullerene derivative is ~ 17 μM) on a freshly cleaved mica surface (~ 1×1 cm) and allowing it to dry under ambient conditions. In the present case, we could observe globular shaped clusters for both the fullerene derivatives (figures 6–8).

By varying the concentration of the fullerene derivatives used for cluster formation, we could observe several types of nanostructures on mica surface. These include, (i) isolated clusters, (ii) larger clusters formed by the association of two or more clusters (figures 6 and 8), and (iii) a three-dimensional network of interconnected clusters (figure 7). Low coverage of clusters allowed us to perform section analysis of individual nanoclusters. The images on the surface of mica are observed as flattened ones and the thickness was measured from the height profile. One of the interesting observations from height profile is that most of these large isolated clusters are formed by the association of smaller clusters (height profiles in figures 6 and 8). For example, in the case of *bis*fullerene derivative (C_{60}–PhA–C_{60}) we could observe smaller clusters and the elongated wire type structure observed on TEM carbon grid is a network of such closely linked spherical fullerene clusters. The structure of a similar molecular system containing two C_{60} units, covalently linked by a cyanine dye was investigated recently using a Scanning tunneling microscope (STM).[32] A self-organized array of molecules was observed by depositing them on a highly oriented pyrolytic graphite (HOPG) surface. We are currently involved in the synthesis of *bis*fullerene derivatives, possessing phenylacetylenes of varying length and further insight on the organization of molecules upon clustering can be obtained by imaging these systems using STM.

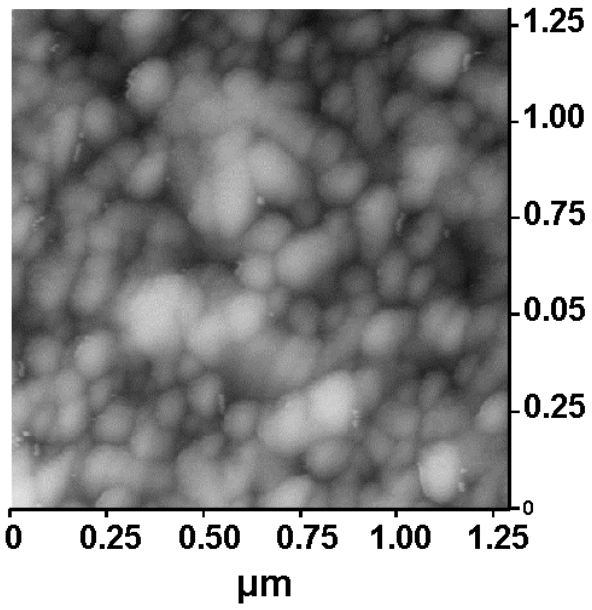

Figure 7. AFM image (*z* range: 400 nm) of thickly packed monofunctionalized fullerene derivative (C_{60}–PhA) assembled on a mica sheet (20 μl of 17 μM cluster solution was transferred to a mica sheet of 1×1 cm).

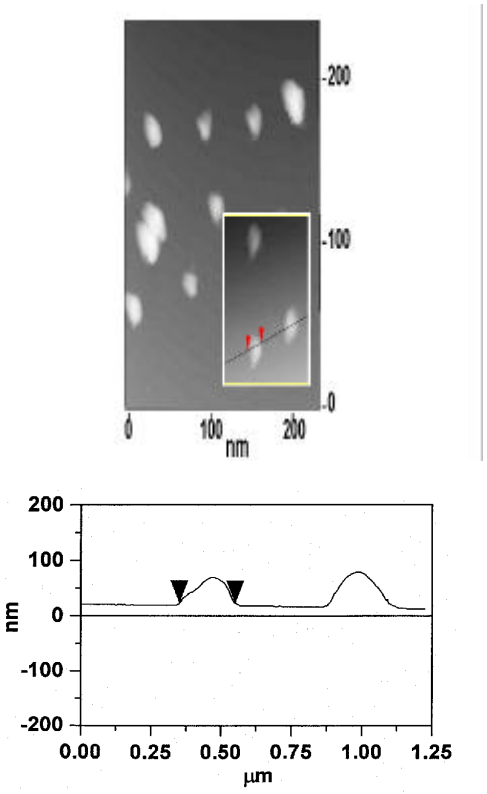

Figure 8. AFM image (*z* range: 400 nm) and sectional analysis of the *bis*fullerene derivative (C_{60}–PhA–C_{60}), assembled on a mica sheet (5 *m*l of 17 *m*M cluster solution was transferred to a mica sheet of 1 × 1 cm).

4. Conclusions

Fullerene derivatives, C_{60}–PhA and C_{60}–PhA–C_{60} form optically transparent clusters absorbing in the UV-Vis region and clustering leads to a significant increase in their molar extinction coefficient. Different nanostructures, which include isolated clusters and network of interconnected clusters, were observed on mica surface by varying the concentration of fullerene derivatives. Height profile studies using AFM indicate that the isolated clusters of C_{60}–PhA–C_{60} are formed by the association of smaller clusters. Dumbbell-shaped *bis*fullerene derivative (C_{60}–PhA–C_{60}) can stack linearly and the elongated wire type structure observed may be a network of closely linked spherical fullerene clusters.

Acknowledgments

This is contribution No RRLT-PPD (PRU)-170 from the Regional Research Laboratory, Trivandrum and NDRL No 4461. The authors (PKS, JPV, KGT and MVG) thank the Council of Scientific and Industrial Research, New Delhi, Department of Science and Technology, Govt. of India, Jawaharlal Nehru Centre for Advanced Scientific Research, Bangalore (MVG) and the Office of Basic Energy Science of the US Department of

Energy (PVK), for financial support of this work. The authors thank Mr. Said Barazzouk for his assistance in the characterization of clusters.

References

1. Varner J E 1988 *Self assembling architecture* (New York: Wiley)
2. Cann A J 1993 *Principle of molecular virology* (San Diego: Academic Press)
3. (a) Lehn J -M 1995 *Supramolecular chemistry concepts and perspectives* (Weinheim: VCH); (b) Piguet C, Bernardinellli G and Hopfgartner G 1997 *Chem. Rev.* **97** 2005; (c) Fujita M, Umemoto K, Yoshizawa M, Fujita N, Kusukawa T and Biradha K 2001 *Chem. Commun.* 509
4. (a) Seidel S R and Stang P J 2002 *Acc. Chem. Res.* **35** 972; (b) Seidel S R and Stang P J 1997 *Acc. Chem. Res.* **30** 502
5. Forster S and Antonietti M 1998 *Adv. Mater.* **10** 195
6. Spatz J P, Roescher A and Moller M 1996 *Adv. Mater.* **8** 337
7. Antonietti M, Forster S, Hartmann J and Oestreich S 1996 *Macromolecules* **29** 3800
8. Moffit M, Mamohjan L, Pessel V and Eisenburg A 1995 *Chem. Mater.* **7** 1185
9. Yue J and Cohen R E 1994 *Supramol. Sci.* **1** 117
10. Goltner C G and Antonietti M 1997 *Adv. Mater.* **9** 1
11. Yang P D, Deng T, Zhao D Y, Feng P Y, Pine D, Chmelka B F, Whitesides G M and Stucky G D 1998 *Science* **282** 2244
12. Goltner C G, Berton B, Kramer E and Antonietti M 1998 *Chem. Commun.* 2287
13. Goltner C G, Berton B, Kramer E and Antonietti M 1999 *Adv. Mater.* **11** 395
14. Wang Y M, Kamat P V and Patterson L K 1993 *J. Phys. Chem.* **97** 8793
15. Sundahl M, Andersson T, Nilsson K, Wennerstrom O and Westman G 1993 *Synth. Methods* **55** 3252
16. Sun Y-P, Ma B, Bunker C E and Liu B 1995 *J. Am. Chem. Soc.* **117** 12705
17. Nath S, Pal H, Palit D K, Sapre A V and Mittal J P 1998 *J. Phys. Chem.* **B102** 10158
18. Sun Y-P, Riggs J E and Liu B 1997 *Chem. Mater.* **9** 1268
19. Thomas K G, Biju V, George M V, Guldi D M and Kamat P V 1999 *J. Phys. Chem.* **B103** 8864
20. Biju V, Barazzouk S, Thomas K G, George M V and Kamat P V 2001 *Langmuir* **17** 2930
21. Biju V, Sudeep P K, Thomas K G, George M V, Barazzouk S and Kamat P V 2002 *Langmuir* **18** 1831
22. Huang S and Tour J M 1999 *Tetrahedron Lett.* **40** 3347
23. Zhou C-Z, Liu T, Xu J-M and Chen Z-K 2003 *Macromolecules* **36** 1457
24. Prato M, Maggini M, Scorrano G and Lucchini V 1993 *J. Org. Chem.* **58** 3613
25. Maggini M, Scorrano G and Prato M 1993 *J. Am. Chem. Soc.* **115** 9798
26. Zhou S, Burger C, Chu B, Sawamura M, Nagahama N, Toganoh M, Hackler U E, Isobe H and Nakamura E 2001 *Science* **291** 1944
27. Horn D and Rieger J 2001 *Angew. Chem., Int. Ed.* **40** 4330
28. Gong X, Milic T, Xu C, Batteas J D and Drain C M 2002 *J. Am. Chem. Soc.* **124** 14290
29. Koti A S R, Periasamy N 2003 *Chem. Mater.* **15** 369
30. Balnois E and Wilkinson K J 2002 *Colloids Surf.* **A207** 229
31. Vinodgopal K, Subramanian V, Carrasquillo S and Kamat P V 2003 *Environ. Sci. Technol.* **37** 761
32. Xiao S, Xu J-H, Li Y-S, Du C-M, Li Y-L, Jiang L and Zhu D 2001 *New J. Chem.* 1610